

## Universality in models for disorder-induced phase transitions

Eduard Vives, Jürgen Goicoechea, Jordi Ortín, and Antoni Planes

*Departament d'Estructura i Constituents de la Matèria, Facultat de Física, Universitat de Barcelona,  
Diagonal 647, E-08028 Barcelona, Catalonia, Spain*

(Received 19 December 1994)

We have systematically analyzed six different reticular models with quenched disorder and no thermal fluctuations exhibiting a field-driven first-order phase transition. We have studied the nonequilibrium transition, appearing when varying the amount of disorder, characterized by the change from a discontinuous hysteresis cycle (with one or more large avalanches) to a smooth one (with only tiny avalanches). We have computed critical exponents using finite size scaling techniques and shown that they are consistent with universal values depending only on the space dimensionality  $d$ .

PACS number(s): 05.50.+q, 64.60.My, 75.60.Ej, 81.30.Kf

Since the proposal of self-organized criticality (SOC) by Bak *et al.* [1] a number of experiments and models have claimed to exhibit such critical behavior. In spite of the initially large number of examples, only a few of them remain clear [2]: these are real earthquakes [3] and some cellular automata models driven by a continuous flux of particles (sandpile models) [4]. When such systems are pulled by a nonlimited external field or flux, they evolve through avalanches which have no characteristic size or duration and thus can be described by power-law distributions [5].

Other examples that were originally presented as realizations of SOC cannot strictly be included in this category since the dynamics through avalanches stops when the external force or field reaches a finite upper or lower value. Nevertheless they share with SOC systems most of the other features. Some of these examples can be included under the common name of “fluctuationless first order phase transitions.” The prototypical example is the behavior of a ferromagnetic material at low temperature under an applied magnetic field [6,7], but similar behavior has been found in athermal martensitic transformations [8], adsorption of liquid He on porous media [9], precipitation of H on Nb [10], and superconductivity in granular Al films [11]. The transition takes place between two phases which are stabilized for very high and very low values of an external applied field. It can be monitored by measuring an order parameter characterizing the amount of each phase (magnetization, amount of martensitic phase, amount of adsorbed He or H, resistivity, etc.). In all these cases, when sweeping the control parameter the order parameter shows hysteresis (which usually does not appear in real SOC systems since the external field cannot be reversed [12]). Hysteresis has almost no temporal dependence and is reproducible from cycle to cycle. As a consequence, in some cases, the interesting “return point memory” effect [12–14] appears. A detailed analysis shows that the evolution proceeds through avalanches joining a sequence of metastable multidomain states. This behavior is a consequence of the existence of disorder in the system and the practical absence of thermal fluctuations. Initially, frozen disorder decides the nucleation of the first domains. This disorder includes magnetic impurities, vacancies, concentration fluctuations, or the random nature of the substrate in the case of adsorption on porous media. After the first nucle-

ation, the following sequence of metastable states can be very complicated. One reason is the existence of forces between domains: magnetic interactions, elastic interactions due to shape or volume changes, etc.; the other is that the disorder itself can change because of the domain evolution. Sometimes the avalanches can be directly observed (Barkhausen effect in ferromagnetic materials [7], acoustic emission in martensitic transformations [15], precipitation of H on Nb [10], and resistivity jumps in superconducting Al films [11], etc.) and some of their properties (size, durations, etc.) characterized. The most striking feature is that the statistical distributions of sizes and durations of the avalanches show power-law behavior which indicates the existence of criticality in a similar way to what happens in real SOC systems. Such avalanche distributions can be characterized by means of “critical exponents.” In this paper we propose that such exponents exhibit universal behavior in analogy with equilibrium critical phenomena. This hypothesis is formulated based on the analysis of a number of models for this phenomena. As will be discussed at the end of this paper, experimental values are still too scarce to test such universality.

Different models can be proposed in order to account for such physical properties. A first set of simple models are the zero temperature ferromagnetic Ising models [14,16] with disorder, defined on a  $d$ -dimensional square lattice with linear size  $L$ . These models are well suited to reproduce the experiments on magnetic systems. The Hamiltonian can be generally written as

$$\mathcal{H} = - \sum_{i,j} S_i S_j - H \sum_i S_i + \mathcal{H}_D, \quad (1)$$

where  $S_i$  is a spin variable taking values  $\pm 1$ , the first sum extends over all nearest neighbor pairs,  $H$  is an external field, and  $\mathcal{H}_D$  is a term including the quenched disorder. At zero temperature, for high values of  $H$  ( $H > H_{max}$ ), the  $+1$  phase is stabilized. When sweeping the field towards lower values, a pure relaxational dynamics (acceptance of all the spin flips decreasing the local energy) will drive the system through a sequence of metastable states, connected by avalanches, until for  $H < H_{min}$  the pure  $-1$  phase is reached. We have used the synchronous dynamics (all unstable spins are updated

simultaneously) which allows one to define independently the size (number of spins reversed) and duration (number of updating steps) for each avalanche [16]. The behavior of the system will depend on the nature and the particular realization of the quenched disorder. We can distinguish two kinds of disorder: random bonds (nonsymmetry breaking terms) which can be written as  $\mathcal{H}_D^J = \sum_{i,j} J_{ij} S_i S_j$ , and random fields (symmetry breaking terms) like  $\mathcal{H}_D^H = \sum_i H_i S_i$ . In order to get extended hysteresis cycles the simplest choice is that  $J_{ij}$  and  $H_i$  have a Gaussian distribution with zero mean and standard deviation  $\sigma_J$  and  $\sigma_H$ , respectively. Possible variations of these models are the change to the antiferromagnetic case, which we have tried and which shows no critical behavior for the avalanche distribution, the change to non-Gaussian distributions of disorder, and the inclusion of interaction to more neighboring cells which could introduce interesting competition phenomena.

A second set of interesting models are the Blume-Emery-Griffiths [17] models with disorder, in which the spins take the three values  $\pm 1, 0$ . They are very promising in describing a first order transition towards a new phase which is degenerated, as happens in thermally induced martensitic transformations. These Hamiltonians can be written as

$$\mathcal{H} = - \sum_{i,j} S_i S_j - K \sum_{i,j} S_i^2 S_j^2 - H \sum_i S_i - \Delta \sum_i S_i^2 + \mathcal{H}_D, \quad (2)$$

where  $K$  is an interaction constant and  $\Delta$  is a field acting on the  $S_i^2$  variables. In addition to the random terms defined previously, two new  $\mathcal{H}_D$  terms are possible:  $\mathcal{H}_D^K = \sum_{i,j} K_{ij} S_i^2 S_j^2$  and  $\mathcal{H}_D^\Delta = \sum_i \Delta_i S_i^2$ , where  $K_{ij}$  and  $\Delta_i$  are random with Gaussian distributions with zero mean and typical deviations  $\sigma_K$  and  $\sigma_\Delta$ , respectively. We generalize the synchronous dynamics choosing, among the three possible states for each variable  $S_i$ , the one minimizing the local energy.

In this paper we present results from a systematic analysis of the random bond (RBIM) and random field (RFIM) Ising models in  $d=2$  and  $d=3$  dimensions and of the downwards (decreasing  $\Delta$ ) and upwards (increasing  $\Delta$ ) transformation in the two-dimensional (2D) random field Blume-Emery-Griffiths model (RFBEG-down and RFBEG-up, respectively) [18] with the disorder terms  $\mathcal{H}_D^\Delta$ ,  $K=1$ , and  $H=0$ . The  $\mathcal{H}_D^\Delta$  for the RFBEG model has been selected to be the simplest one which is different from the  $\mathcal{H}_D$  used in the Ising models.

For each model we have studied the hysteresis loop of the order parameter ( $m = \sum S_i$  or  $M = \sum S_i^2$ ) when the external field ( $H$  or  $\Delta$ ) is swept from  $+\infty$  to  $-\infty$  and back. Figure 1 shows as an example results for the 2D RBIM. For small values of the standard deviation of the disorder distribution  $\sigma$ , the hysteresis loops show a discontinuous jump (size proportional to  $L^d$ ) while for a larger amount of disorder the loops are smooth (formed by a sequence of tiny jumps). This behavior is acknowledged to be a nonequilibrium phase transition induced by the amount of disorder  $\sigma$  [14,16]. Different parameters can be measured and averaged ( $\langle \dots \rangle_L$ ) over a set of replicas of the system corresponding to different realizations of the random distribution of bonds or fields. The transition takes place at a value of the disorder ( $\sigma_c(L)$ )

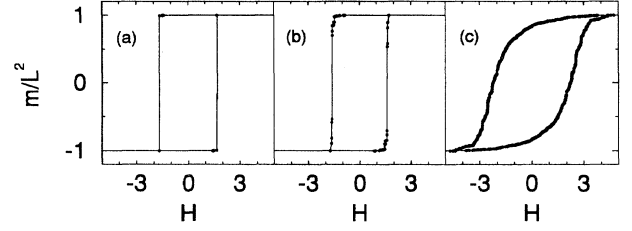


FIG. 1. Hysteresis cycles corresponding to the 2D RBIM for three different values of the amount of disorder  $\sigma$ , obtained by numerical simulation of a system with size  $L=40$ : (a)  $\sigma=0.45 < \sigma_c(L)$ ; (b)  $\sigma=0.55 \approx \sigma_c(L)$ ; (c)  $\sigma=1.5 > \sigma_c(L)$ .

where the mean size of the largest avalanche in the hysteresis cycle ( $\langle m_0 \rangle_L$ ) shows an inflexion, the mean duration of the largest avalanche ( $\langle t_0 \rangle_L$ ) shows a maximum, and the distribution of avalanche sizes  $[p_L(m)]$  shows power-law behavior. Actually,  $\sigma_c(L)$  is not the same for the singular behavior in the three magnitudes, but tends to a unique value  $\sigma_c$  for  $L \rightarrow \infty$ . For the infinite system, inspired on the usual equilibrium critical phenomena relations, we assume that

$$\xi \sim \left| \frac{\sigma_c - \sigma}{\sigma_c} \right|^{-\nu}, \quad (3)$$

$$\langle m_0 \rangle / L^d \sim \xi^{-\beta} \sim \left( \frac{\sigma_c - \sigma}{\sigma_c} \right)^{\beta\nu} \quad \text{for } \sigma < \sigma_c, \quad (4)$$

$$\langle t_0 \rangle \sim \xi^z \sim \left| \frac{\sigma_c - \sigma}{\sigma_c} \right|^{-\nu z}, \quad (5)$$

$$p(m) \sim m^{-\tau}, \quad (6)$$

where  $\xi$  is the correlation length and  $\nu$ ,  $\beta$ ,  $z$ , and  $\tau$  are critical exponents characterizing the transition. They can be obtained from numerical simulations of finite systems assuming finite size scaling relations:  $\langle m_0 \rangle_L / L^{d+\beta}$  and  $\langle t_0 \rangle_L / L^z$  should scale when represented as a function of the scaling variable  $L^{1/\nu}(\sigma - \sigma_c(L)) / \sigma_c(L)$ . The relation of the scaling properties of the replica averages for a finite system with the behavior of a single system in the thermodynamic limit for such a nonequilibrium problem is, to our knowledge, not clearly established. A possible connection may go along the lines of a recently proposed dynamical model for spin glasses [19]. The details of the procedure used to fit the exponents and the extrapolation to the infinite system are given in [14] for the case of the 3D RFIM and in [16] for the case of the 2D RBIM. In Fig. 2, we present, as another example, results for the RFBEG-down and RFBEG-up models: the scaling of  $\langle t_0 \rangle_L$  and  $\langle m_0 \rangle_L$ , the behavior of  $\sigma_c(L)$ , and the critical distributions of the avalanches  $p(m)$  are shown. A summary of the results for the six models mentioned above is presented in Table I. They have been obtained by numerical simulations of systems of sizes up to  $L=100$  and averaging over  $\sim 500$  replicas. Values within parentheses are taken from the data in Ref. [14]. Error bars are very conservative, including the deviations arising from different fitting (linear or logarithmic) and scaling methods (using the height or the curvature of  $\langle t_0 \rangle_L$  and the height or slope of  $\langle m_0 \rangle_L$ ).

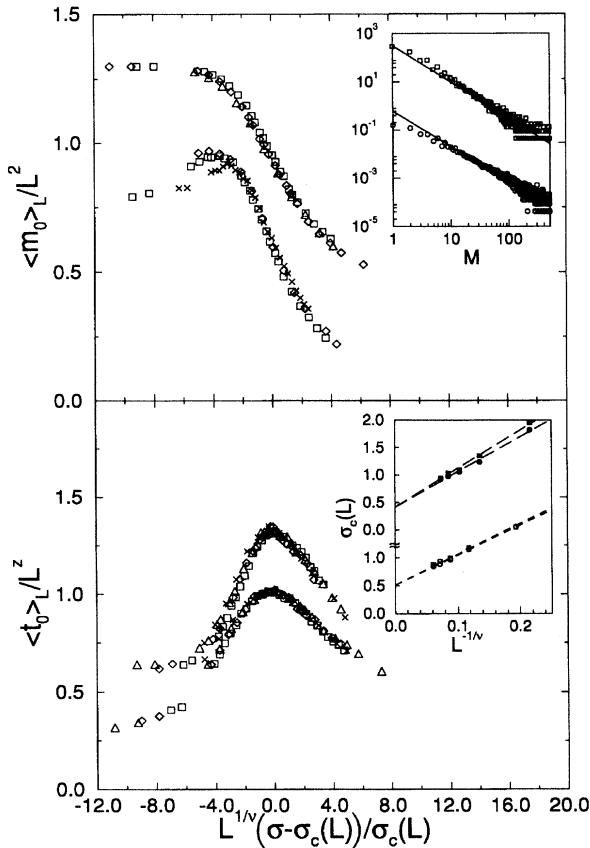


FIG. 2. Results for the RFBEg-down and RFBEg-up (shifted-up) models. We show the behavior of  $\langle m_0 \rangle_L / L^2$  (a) and  $\langle t_0 \rangle_L / L^z$  (b) vs the scaling variable. The different symbols correspond to  $L=20$  ( $\square$ ),  $30$  ( $\diamond$ ),  $40$  ( $\triangle$ ), and  $50$  ( $\times$ ). The inset above shows the behavior of the critical distribution of avalanches with the power-law fit, and the inset below the dependence of  $\sigma_c(L)$ , computed using the inflexion in  $\langle m_0 \rangle_L$  ( $\square$ ) and the maximum in  $\langle t_0 \rangle_L$  ( $\circ$ ), in front of  $L^{-1/\nu}$ .

The results are compatible with the existence of a set of universal values for the exponents, only depending on the lattice dimensionality.

The same exponent values have been obtained for random bonds and random fields, although it is known that these two

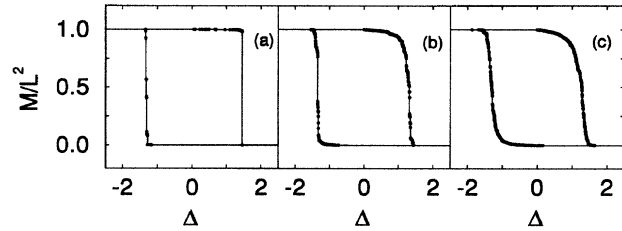


FIG. 3. Hysteresis cycles corresponding to the 2D RFBEg model for three different values of the amount of disorder  $\sigma$ , obtained by numerical simulation of a system with size  $L=100$ : (a)  $\sigma=0.6 < \sigma_c(L)^{up}$ ; (b)  $\sigma=0.8$ ; (c)  $\sigma=1.3 > \sigma_c(L)^{down}$ .

ways of introducing disorder affect differently the standard critical phenomena [20]. It is worthwhile to notice that the different disorder terms in the Hamiltonians (1) and (2) exhibit different symmetry properties under the change  $S_i \rightarrow -S_i$ . As a consequence, the two branches of the hysteresis cycle are exactly symmetric for the RBIM, statistically symmetric for the RFIM, and not symmetric for the RFBEg model. For this last model the upward and downward branches of the hysteresis cycle show critical behavior at different  $\sigma_c$ . This can be seen in Fig. 3 where a sequence of hysteresis cycles corresponding to different  $\sigma$  is displayed. The downward branch corresponds to a jump from a pure 0 phase to a degenerated phase with mixed 1 and  $-1$ , while the upward branch corresponds to a jump from the degenerated phase to the 0 phase.

Two points about the numerical values of the exponents should be made. First, the value of the exponent  $\beta$  for the dependence of the size of the biggest avalanche when approaching  $\sigma_c$  is very small, and the statistical uncertainties do not enable us to discard a value of  $\beta=0$  (scaling in Fig. 2 has been done using  $\beta=0$ ). The same has been found by other authors [21] for the RFIM in  $d=3$ . Second, the values of the exponent  $\tau$  for the critical distribution of avalanche sizes (corresponding to a complete branch) fit well with the relation  $\tau=2 - [(5-d)/(2d+2)]$  for the integrated distribution of avalanches in the depinning transition [22]. Indeed, the local advance of the avalanches in the fluctuationless first-order phase transitions is closely related to the depinning problem [23] but, to our knowledge, there is a lack of a detailed exact mapping.

TABLE I. Critical exponents from zero temperature simulations of the disorder induced phase transition for the RBIM, the RFIM, and the RFBEg in 2D and 3D. Values in parentheses correspond to Ref. [14].

Exponent	2D				3D	
	RFIM	RBIM	RFBEg-down	RFBEg-up	RFIM	RBIM
$z$	$1.3 \pm 0.1$	$1.2 \pm 0.1$	$1.3 \pm 0.1$	$1.2 \pm 0.1$	$1.6 \pm 0.1$	$1.6 \pm 0.1$
$\nu$	$1.6 \pm 0.1$	$1.4 \pm 0.1$	$1.4 \pm 0.1$	$1.5 \pm 0.1$	$1.15 \pm 0.1$ ( $1.0 \pm 0.1$ )	$1.06 \pm 0.1$
$D = \beta + d$	$2.2 \pm 0.2$	$2.0 \pm 0.1$	$2.2 \pm 0.2$	$2.4 \pm 0.4$	$3.0 \pm 0.1$ ( $3.17 \pm 0.07$ )	$3.0 \pm 0.1$
$\tau$	$1.3 \pm 0.2$	$1.45 \pm 0.1$	$1.3 \pm 0.1$	$1.5 \pm 0.1$	$1.8 \pm 0.1$ ( $2.03 \pm 0.03$ )	$2.0 \pm 0.2$
$\sigma_c$	$0.75 \pm 0.03$	$0.44 \pm 0.03$	$0.51 \pm 0.03$	$0.42 \pm 0.02$	$2.18 \pm 0.08$ ( $2.25 \pm 0.05$ )	$1.12 \pm 0.05$

Comparison of the simulation values with the experimental ones is difficult. First, although the critical region for these systems is large [21], it might well be that the measured exponents are modified by the existence of an exponential prefactor to the power law. To elucidate this point, data extending over several decades would be required. Second, the measured exponents correspond to distributions of magnitudes that are related to the avalanche size [ $p(m) \sim m^{-\tau}$ ] but not always in a known way. For experiments on reversal of magnetic domains [6], a value of 2.5 for the distribution of avalanche “sizes” has been found by optical photography. In fact, such measured sizes are not directly related to the real avalanche sizes. For martensitic transformations [8] a value of  $\sim 3$  has been found for the distribution of amplitudes of acoustic emission signals. The

relation between these amplitudes and avalanche sizes is still unclear. The same happens for the value of 1.9 measured from the acoustic emission generated by the cracks produced by H precipitation in Nb [10]. These few examples show the diversity of physical magnitudes measured and techniques used in the experimental search for power-law distributions in real systems. We believe that an experimental test of the universality proposed in this work will only be possible when many different systems are interrogated for the same physical magnitudes.

We acknowledge fruitful discussions with L. Tang. We also acknowledge financial support from the Comisión Interministerial de Ciencia y Tecnología (CICYT, project number MAT92-884).

- 
- [1] P. Bak, C. Tang, and K. Wiesenfeld, *Phys. Rev. Lett.* **59**, 381 (1987); *Phys. Rev. A* **38**, 364 (1988).
- [2] D. Sornette, *J. Phys. (Paris)* **4**, 209 (1994).
- [3] Z. Olami, H. J. S. Feder, and K. Christensen, *Phys. Rev. Lett.* **68**, 1244 (1992); A. Sornette and D. Sornette, *Europhys. Lett.* **9**, 197 (1989).
- [4] K. Wiesenfeld, J. Theiler, and B. McNamara, *Phys. Rev. Lett.* **65**, 949 (1990).
- [5] S. Maslov, M. Oaczuski, and P. Bak, *Phys. Rev. Lett.* **73**, 2162 (1994).
- [6] K. L. Babcock and R. M. Westervelt, *Phys. Rev. Lett.* **64**, 2168 (1990).
- [7] P. J. Cote and L. V. Meisel, *Phys. Rev. Lett.* **67**, 1334 (1991).
- [8] E. Vives, J. Ortín, Ll. Mañosa, I. Ràfols, R. Pérez-Magrané, and A. Planes, *Phys. Rev. Lett.* **72**, 1694 (1994).
- [9] M. P. Lilly, P. T. Finley, and R. B. Hallock, *Phys. Rev. Lett.* **71**, 4186 (1993).
- [10] G. Cannelli, R. Cantelli, and F. Cordero, *Phys. Rev. Lett.* **70**, 3923 (1993).
- [11] W. Wu and P. W. Adams, *Phys. Rev. Lett.* **74**, 610 (1995).
- [12] A reversible cellular automaton with hysteresis is proposed by J. Goicoechea and J. Ortín, *Phys. Rev. Lett.* **72**, 2203 (1994).
- [13] J. Ortín, *J. Appl. Phys.* **71**, 1456 (1992).
- [14] J. P. Sethna, K. Dahmen, S. Kartha, J. A. Krumhansl, B. W. Roberts, and J. D. Shore, *Phys. Rev. Lett.* **70**, 3347 (1993); K. Dahmen and J. P. Sethna, *ibid.* **71**, 3222 (1993); J. P. Sethna, K. Dahmen, S. Kartha, J. A. Krumhansl, O. Perković, B. W. Roberts, and J. D. Shore, *ibid.* **72**, 947 (1994).
- [15] A. Planes, J. L. Macqueron, M. Morin, and G. Guénin, *Phys. Status Solidi A* **66**, 717 (1981).
- [16] E. Vives and A. Planes, *Phys. Rev. B* **50**, 3839 (1994).
- [17] M. Blume, V. J. Emery, and R. B. Griffiths, *Phys. Rev. A* **4**, 1071 (1971).
- [18] J. Goicoechea and J. Ortín, *J. Phys. IV* **5**, C2-71 (1995).
- [19] A. C. Coolen, R. W. Penney, and D. Sherrington, *Phys. Rev. B* **48**, 16 116 (1993).
- [20] Y. Imry and S. K. Ma, *Phys. Rev. Lett.* **35**, 1399 (1975); Y. Imry and M. Wortis, *Phys. Rev. B* **19**, 3580 (1979); A. N. Berker, *Physica A* **194**, 72 (1993); A. N. Berker and A. Falicov, *Turk. J. Phys.* **18**, 347 (1994).
- [21] K. Dahmen, O. Perković, and J. P. Sethna, to be published (1994).
- [22] L. Tang (private communication).
- [23] O. Narayan and D. S. Fisher, *Phys. Rev. B* **46**, 11 520 (1992); **48**, 7030 (1993).